

## FORMATION OF OPTICAL LINES IN BLACK-HOLE BINARIES

KINWAH WU,

*School of Physics, University of Sydney, NSW 2006, Australia and  
 Mullard Space Science Laboratory, University College London,  
 Holmbury St. Mary, Dorking, Surrey RH5 6NT, United Kingdom,  
 E-mail: kw@mssl.ucl.ac.uk*

ROBERTO SORIA,

*Mullard Space Science Laboratory, University College London,  
 Holmbury St. Mary, Dorking, Surrey RH5 6NT, United Kingdom,  
 E-mail: rs1@mssl.ucl.ac.uk*

HELEN JOHNSTON AND RICHARD HUNSTEAD

*School of Physics, University of Sydney, NSW 2006, Australia  
 E-mail: helenj@physics.usyd.edu.au, rwh@physics.usyd.edu.au*

The H I Balmer emission lines of black-hole binaries show double-peaked profiles during the high-soft state and the quiescent state. In the high-soft state the profiles are asymmetric with a stronger red peak, but the profiles are symmetric in the quiescent state. We suggest that in the high-soft state the emission lines originate from the temperature-inversion layer caused by irradiative heating of an optically thick accretion disk. Irradiative heating also causes the formation of a disk wind, which mildly absorbs the blue peak of the lines. The double-peaked lines seen in the quiescent state arise from an optically thin disk. In the absence of a disk wind, the lines are unabsorbed and so the symmetry of the line profiles is preserved.

## 1 Background

Many soft X-ray transients are probably close binary systems containing a black hole accreting material from a low-mass companion star. These systems often show three distinctive X-ray spectral states, which are commonly classified as the high-soft state, the low-hard state and the quiescent state (see e.g. review by Tanaka and Lewin<sup>1</sup>). The high-soft state is characterised by a prominent blackbody-like thermal component and high-energy power-law tail in the X-ray spectrum. The effective temperature of the thermal component is  $\sim 1$  keV. The slope of the power-law is steep, with a photon index  $\Gamma \sim 2-4$ , and it can extend to energies beyond 100 keV. The thermal component is generally insignificant in the low-hard state. The X-ray spectrum is dominated by a power-law component, but the photon index of the power-law (typically  $\sim 1-2$ ) is significantly flatter than that of the high-soft state.

There is strong observational evidence that the morphology of the optical emission lines changes with the X-ray spectral properties<sup>2</sup>. For instance, it was found that the equivalent widths of H I Balmer emission lines correlated with the hard (20–100 keV) X-ray luminosity during the hard X-ray outbursts of GRO J1655–40<sup>3</sup>. This correlation was, however, not found for the He II lines<sup>3</sup>. Another example is that the H I Balmer emission lines of black-hole binaries generally have double-peaked profiles in the high-soft state<sup>4</sup>. The two peaks are asymmetric, with the red peak stronger than the blue peak. It also appears that the double-peaked lines are

in superposition with a broader absorption trough<sup>3</sup>. This is contrary to the situation in the low-hard state, when the H I Balmer lines are more often single-peaked<sup>4</sup>. Interestingly, when the systems are in quiescence the lines are also double-peaked (e.g. A0620–00), but unlike the asymmetric profiles seen in the high-soft state, the line profiles tend to be very symmetric<sup>5</sup>.

## 2 Formation of double-peaked lines

A direct interpretation is that the double-peaked lines arise from the accretion disk<sup>6</sup>. The red and blue peaks come from the disk regions with receding and approaching line-of-sight velocities respectively. When the system is X-ray active, it is also optically bright, with the optical continuum dominated by the disk emission. The optical emission region in the accretion disk is probably opaque, as the optical continuum seems to be well fitted by a thermal blackbody model<sup>7</sup>.

The standard theories of radiative transfer (see e.g. Mihalas<sup>8</sup>, Tucker<sup>9</sup>) predict a smooth thermal spectrum for the emission from an opaque, isothermal medium. The spectrum would show absorption line features if there is a negative temperature gradient towards the surface. Emission lines are formed only when the brightness temperature at the line-centre energies is higher than the thermal temperature of the nearby continuum. If the medium is opaque to the continuum, this implies that the lines are formed in the presence of a temperature-inversion surface layer. This is analogous to the spectra of OB stars, which are dominated by absorption lines, and the spectra of cooler G and K stars, which show strong emission lines. When the medium is transparent to the continuum, the spectrum will show emission lines, because the line opacities are generally higher than continuum opacities.

If we accept the view that the accretion disks in black-hole binaries are opaque to optical emission in the X-ray active state, then the double-peaked optical lines seen in the high-soft state suggest the presence of a temperature-inversion layer on the accretion-disk surface. The disappearance of the double-peaked profiles in the low-hard state may be due either to the fact that the geometry of the accretion disk—and hence its optical depth—is modified<sup>2</sup>, or that the line emission is dominated by a non-disk component. The double-peaked lines seen in the quiescent state are probably emission from a low-density accretion disk optically thin to the continuum. We now examine this scenario in more detail.

## 3 Line formation in an opaque accretion disk

### 3.1 A plane-parallel model

We use a simple plane-parallel model<sup>10</sup> to illustrate that a temperature-inversion layer can be set up on the surface of an accretion disk under soft X-ray illumination. The model is a modification of that proposed by Milne<sup>11</sup> for irradiative heating of the atmosphere of a star by its companion. The geometry of the model is shown in Figure 1. The basic assumptions in the model are (i) the emission region is semi-infinite and planar, (ii) the accretion disk is in radiative equilibrium, and (iii) the process is linear. In addition, we also assume that the cooling is dominated by

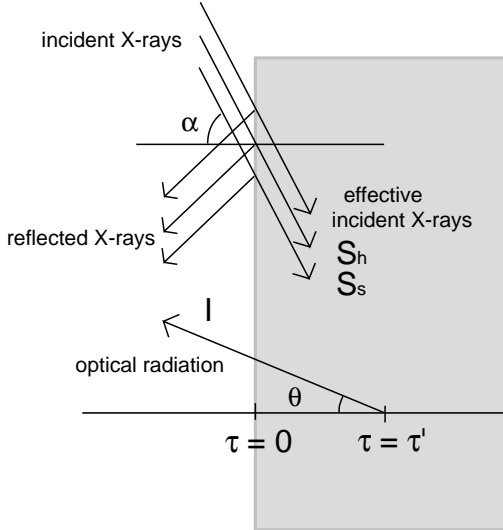


Figure 1. The geometry of the plane-parallel model. The disk surface is placed vertically and is illuminated by soft and hard X-rays at an incident angle  $\alpha$ .

the optical continuum emission.

As the radiative-transfer equations are linear under these assumptions, the temperature  $T$  at an optical depth  $\tau$  is given by

$$T(\tau) = \left[ \frac{\pi}{\sigma} \left( B_x(\tau) + B_d(\tau) \right) \right]^{1/4} \equiv \left[ \frac{\pi}{\sigma} B(\tau) \right]^{1/4}, \quad (1)$$

where  $\sigma$  is the Stefan-Boltzmann constant,  $B_x(\tau)$  is the component of the radiation due to irradiative heating, and  $B_d(\tau)$  is the component due to viscous heating in the absence of X-ray irradiation. The disk component<sup>13</sup> is

$$B_d(\tau) = \frac{3}{4} S_d \left[ \tau \left( 1 - \frac{\tau}{2\tau_{\text{tot}}} \right) + \frac{2}{3} \right], \quad (2)$$

where  $\tau_{\text{tot}}$  is the total opacity of the accretion disk in the direction perpendicular to the disk surface, and  $S_d = \sigma T_{\text{eff}}^4 / \pi$  is the viscous energy flux from the disk mid-plane<sup>12</sup>. The effective temperature  $T_{\text{eff}}$ , which is determined by balancing the energy generated by viscous heating and by radiative loss, is given roughly by

$$\sigma T_{\text{eff}}^4 \approx \frac{9}{8} \nu \Sigma \Omega_K^2, \quad (3)$$

where  $\nu$  is the viscosity coefficient,  $\Sigma$  is the surface density of the disk, and  $\Omega_K$  is the Keplerian angular velocity.

Suppose the incident radiation consists of parallel beams of soft and hard X-rays, with effective fluxes  $\pi S_h$  and  $\pi S_s$  per unit area normal to the beams, and making an angle  $\alpha$  with the normal to the disk plane. The beams are absorbed exponentially, with the absorption coefficient of the soft X-rays  $k_s \kappa$ , and that of

the hard X-rays  $k_h \kappa$ , where  $\kappa$  is the absorption coefficient of the optical radiation. Radiative equilibrium requires the rate of energy absorption be equal to the rate of radiative cooling. It implies that

$$\pi(k_s S_s e^{-k_s \tau \sec \alpha} + k_h S_h e^{-k_h \tau \sec \alpha}) + \int_{4\pi} d\Omega I(\tau, \mu) = 4\pi B_x(\tau), \quad (4)$$

where  $I(\tau, \mu)$  is the intensity of the optical radiation from the irradiatively heated disk at the depth  $\tau$  in the direction  $\theta (= \cos^{-1} \mu)$ . On the other hand, by multiplying the radiative-transfer equation

$$\mu \frac{d}{d\tau} I(\tau, \mu) = I(\tau, \mu) - B_x(\tau) \quad (5)$$

by a differential solid angle  $d\Omega$ , integrating with respect to  $\tau$  and using the condition of radiative equilibrium, we obtain

$$\int_{4\pi} d\Omega \mu I(\tau, \mu) = \pi \cos \alpha (S_s e^{-k_s \tau \sec \alpha} + S_h e^{-k_h \tau \sec \alpha}). \quad (6)$$

For the condition of no inward component of  $I(\tau, \mu)$  at the boundary ( $\tau = 0$ ),

$$\int_{-1}^0 d\mu I(0, \mu) = 0 \quad (7)$$

and

$$\int_{-1}^0 d\mu \mu I(0, \mu) = 0. \quad (8)$$

If we define a hardness parameter  $\xi \equiv S_h/S_s$  and a total X-ray flux  $S_x \equiv S_s + S_h$ , then by solving all the equations above with the two boundary conditions, we have

$$B_x(\tau) = \frac{1}{2} S_x \left\{ k_s f_s(\alpha) \left( \frac{\xi}{1+\xi} \right) \left[ \left( \frac{\cos \alpha}{k_s} \right) - \left( \frac{\cos \alpha}{k_s} - \frac{1}{2} \right) e^{-k_s \tau \sec \alpha} \right] + k_h f_h(\alpha) \left( \frac{1}{1+\xi} \right) \left[ \left( \frac{\cos \alpha}{k_h} \right) - \left( \frac{\cos \alpha}{k_h} - \frac{1}{2} \right) e^{-k_h \tau \sec \alpha} \right] \right\}. \quad (9)$$

where the functions  $f_s(\alpha)$  and  $f_h(\alpha)$  are given by

$$f_{s,h}(\alpha) = \left[ 1 - \left( \frac{\cos \alpha}{k_{s,h}} \right) + \left( \frac{\cos \alpha}{k_{s,h}} \right) \left( \frac{\cos \alpha}{k_{s,h}} - \frac{1}{2} \right) \ln(1 + k_{s,h} \sec \alpha) \right]^{-1}. \quad (10)$$

### 3.2 Temperature-inversion layer

In Figure 2 we show the temperature as a function of the optical depth for annuli of accretion disks illuminated by soft and hard X-rays at an incident angle of  $87^\circ$ . When the disk is illuminated by soft X-rays, if the X-ray flux is larger than the viscous heat flux emerging from the disk mid-plane, a temperature-inversion layer can be set up. If the X-ray flux is weak, the temperature gradient remains negative, implying that irradiative heating is unimportant and the temperature structure is determined mainly by the transport of the energy generated deep in the disk mid-plane by viscous heating. Moreover, the temperature inversion is stronger for

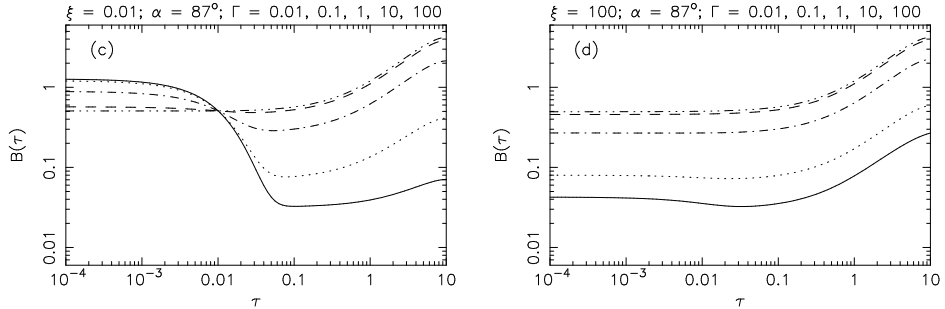


Figure 2. (Left) Temperature profile ( $T \propto B^{1/4}$ ) as a function of optical depth  $\tau$  for an X-ray incident angle  $\alpha = 87^\circ$  and an hardness parameter  $\xi = 0.01$  (i.e. strong soft X-ray illumination). The two scaling parameters for the X-ray opacities are  $k_s = 5.0$  and  $k_h = 0.01$ , and the total optical depth  $\tau_{\text{tot}} = 20$ . The total flux density is normalised such that  $S_x + S_d = 1.0$ . The curves correspond to illumination-strength parameters  $\tilde{\Gamma} \equiv S_x/S_d = 100$  (solid line), 10 (dotted line), 1 (dash-dotted line), 0.1 (dashed line) and 0.01 (dash-dot-dot-dotted line). (Right) Same parameters as those in the left panel except  $\xi = 100$  (i.e. strong hard X-ray illumination).

larger incident angles of the X-rays<sup>10</sup>. When the disk is illuminated by hard X-rays, the disk always has a negative temperature gradient, and no strong temperature inversion occurs.

Opacities are usually larger for soft X-rays ( $\sim 0.1 - 1$  keV) than for the optical continuum radiation, and hence soft X-rays are more easily absorbed by the disk. When a significant amount of energy is deposited at a small depth below the disk surface, a temperature inversion is formed. Harder X-rays ( $\sim 10$  keV), which are absorbed only in dense media, tend to deposit energies deep below the disk surface. As a result, the disk is heated uniformly under hard X-ray illumination.

In Figure 3 we show the location of disk regions at which temperature inversion occurs for systems with an accreting black hole of  $7 M_\odot$  and a modest accretion rate of  $5 \times 10^{17} \text{ g s}^{-1}$ . The X-rays illuminate the accretion disk at a grazing incident angle of  $87^\circ$  and a substantial portion of the X-rays are reflected. If the X-rays are hard (middle panel) and the reflection is large (99%), no strong temperature inversion can be set up at all distances from the central black hole. The temperature structures in the inner disk regions ( $R < 10^{10} \text{ cm}$ ) are not significantly affected by irradiative heating. The temperatures of the outer disk regions ( $R > 10^{10} \text{ cm}$ ), however, increase substantially. For smaller reflection (50%) and softer X-rays (right panel), a weak temperature inversion is set up at distances larger than  $\sim 10^9 \text{ cm}$  from the black hole, and the temperature structure of the disk region beyond  $R \sim 10^8 \text{ cm}$  is greatly modified.

If the X-rays are soft and the reflection is large, a strong temperature inversion can be set up over a substantial fraction of the area of the accretion disk (left panel, Fig. 3). While the temperature structures of the inner disk regions are still determined by viscous heating, those of the outer disk rim are determined by irradiative heating. The predicted temperature of the temperature-inversion layer at  $R \sim 10^{11} \text{ cm}$  is about  $10^4 - 10^5 \text{ K}$ . This is indeed the temperature at which

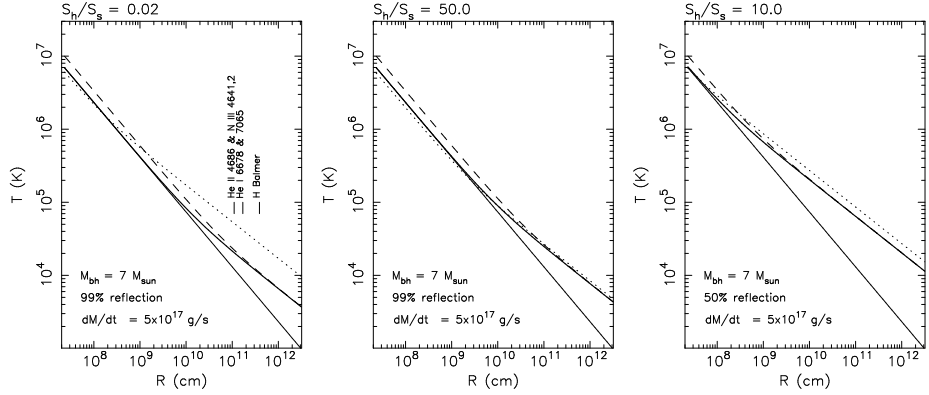


Figure 3. The temperature structures of an irradiatively heated accretion disk calculated from the plane-parallel model. The surface temperature (at  $\tau = 0$ ) of the disk is represented by the dotted line; the effective temperature (at  $\tau = 2/3$ ) by the thick solid line; and the temperature at  $\tau = 10$  by the dashed line. We have assumed a Shakura-Sunyaev disk with a viscosity parameter  $\alpha_{\text{vis}} = 1$ . For comparison we also show the effective temperature (thin solid line) of the same Shakura-Sunyaev disk without X-ray irradiation. The mass of the black hole is  $7 M_{\odot}$ ; the mass-accretion rate is  $5 \times 10^{17} \text{ g s}^{-1}$ ; and the incident angle of the X-rays is fixed to be  $87^\circ$ . In the left panel, the disk is irradiated by X-rays with a hardness ratio  $\xi = 0.02$ , and 99% of the X-rays are reflected. We mark the radii at which the Balmer, He I  $\lambda 6678$ , He I  $\lambda 7065$ , He II  $\lambda 4686$  and N III  $\lambda\lambda 4641,4642$  lines are emitted, inferred from the peak separation observed from GX 339–4 in 1998. In determining the location of the line-emission region, we assume an orbital inclination  $i$  of  $15^\circ$  and that the lines are emitted from a geometrically thin, Keplerian accretion disk. If the period is longer or the orbital inclination is larger, the line-emission regions will be at some larger radii. H I Balmer lines are emitted at temperatures  $\sim (1 - 2) \times 10^4 \text{ K}$ ; He I lines at  $\sim (2 - 4) \times 10^4 \text{ K}$ ; and He II lines at  $\sim (5 - 10) \times 10^4 \text{ K}$ . The Bowen N III  $\lambda\lambda 4641,4642$  lines are formed in regions where He II  $\lambda 304$  photons are abundant. As shown, the temperatures at the inversion layer are consistent with the temperatures at which these lines are emitted. In the middle panel, the accretion disk is irradiated by X-rays with a hardness ratio of  $\xi = 50$ , and 99% of the X-rays are reflected. In the right panel, the hardness ratio  $\xi = 10$ , and only 50% of the X-rays are reflected.

the optical H and He lines are expected to form (see e.g. Cox and Tucker<sup>14</sup>, and Osterbrock<sup>15</sup>). The distances predicted by the model ( $R \sim 10^{11} \text{ cm}$ ) are in good agreement with the observed peak-separation of GX 339–4 (left panel, Fig. 3) for an orbital period<sup>16</sup> of 15 h and an orbital inclination<sup>10</sup> of  $15^\circ$ .

## 4 Line morphology

### 4.1 Asymmetric profiles and absorption troughs

The main characteristics of the optical double-peaked lines of black-hole binaries seen in the high-soft states are that (i) the peaks are asymmetric with a stronger red peak and (ii) the lines are associated with broad absorption troughs. As shown in the sections above, irradiative heating can cause an increase in the local temperature of the accretion disk. If the thermal temperature of the disk surface at a radius  $R$  is significantly larger than the local virial temperature, the disk material at the

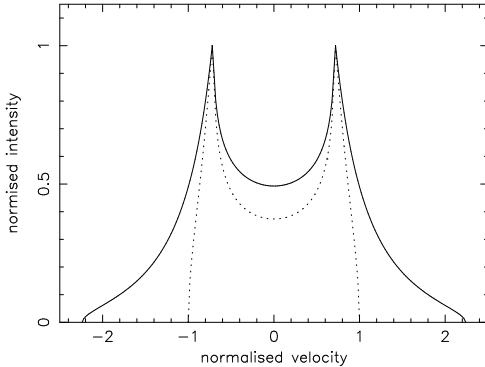


Figure 4. Normalised profiles of double-peaked lines from an optically thin, viscous heated disk (solid line) and an irradiatively heated accretion disk (dotted line). For the viscous heated disk, radiation is emitted throughout the entire viscous heated disk, with a emissivity function of a second-order power law of the disk radius. For the irradiatively heated disk, only the outer disk regions, where temperature inversion occurs, emit line radiation. Here the inner radius of the heated region is assumed to be half of the accretion-disk radius, and the emissivity function take the same power-law form. The viewing angles in both cases are  $45^\circ$ . The line of the viscous heated disk has a standard Smak<sup>6</sup> profile, but the line of the irradiatively heated disk does not. Note that there is a significant difference in the wings of the two lines.

surface will evaporate. Irradiative heating is more effective at larger radii and a wind will be formed in the outer disk regions with velocities slightly higher than the local virial (and Keplerian) velocities. Because the wind is from the outer disk, the temperatures are not necessarily very high. The wind, which always has negative line-of-sight velocities with respect to a distant observer, absorbs only the blue part of the lines. As the wind does not absorb the red part of the line, the lines appear to have a stronger red peak.

The broad absorption troughs are due to the absorption of the continuum by high-velocity material. If the broad absorption lines originate from the accretion disk, X-ray irradiative heating should be unimportant in the regions where they are formed. A natural choice is that the absorption regions are at smaller radii than the regions where temperature inversion occurs. This is consistent with the observations that the absorption troughs are broader than the double-peaked emission lines formed in the temperature-inversion layer.

#### 4.2 Temperature-inversion vs optically thin disk

For an irradiatively heated accretion disk, the emission lines arise from the temperature-inversion layer in the outer disk region. As the inner disk region, where the Keplerian velocities are large, does not contribute to the line emission, the lines should have weak wings. Figure 4 illustrates the difference between the line wings of an irradiatively heated disk and a conventional accretion disk, for which the line assumes a Smak<sup>6</sup> profile. If the emissivity of the line emission regions have the same dependence on the radius, the line profile of the irradiatively heated disk

has weaker wings and sharper peaks.

If the accretion disk is optically thin to the optical continuum, the line emission regions may cover a large portion of the accretion disk, which includes the inner disk region. As substantial emission is contributed by the high-velocity material in the inner disk region, the lines would have strong wings. As the accretion disk does not have a strong wind to absorb the line, the line profiles preserve the symmetry of the red and blue peaks. Observations<sup>5</sup> show that the H I Balmer line profiles of A0620-00 in quiescence are consistent with the theoretical Smak<sup>6</sup> profiles. The different morphology of the doubled-peaked Balmer lines observed in RXTE J1550-564, GX 339-4 and GRO J1655-40 during the high-soft state and the lines observed in A0620-00 during quiescence supports the interpretation that emission lines are formed in a temperature-inversion layer above an opaque accretion disk when the system is in the high-soft state, and emission lines are formed in the disk regions transparent to the optical continuum when the system is in an X-ray quiescent state.

## 5 Summary

Black-hole binaries show double-peaked emission lines during the high-soft and X-ray quiescent states. The line profiles observed in the high-soft state are asymmetric with a stronger red peak. Moreover, the lines are often associated with broad absorption. The emission lines are probably formed in a temperature-inversion layer on the surface of an accretion disk optically thick to the optical continuum. The temperature-inversion layer is due to irradiative heating from regions near the accreting black holes. Strong temperature inversion can be formed only when the X-rays have a strong soft ( $\sim 0.1 - 1$  keV) component. Irradiation by only hard ( $\sim 10$  keV) X-rays heats the disk uniformly at all depths, and will not lead to the formation of the temperature-inversion layer. Irradiative heating by soft X-rays may also cause the evaporation at the surface of the outer disk, and hence drive a wind. Because of the approaching line-of-sight velocities, the wind preferentially absorbs the blue part of the lines, causing the asymmetry in the line profiles.

The double-peaked lines observed in the quiescent state are highly symmetric and have strong wings, consistent with a theoretical Smak profile. As an opaque medium with no temperature variations along the optical path, or with a negative temperature gradient, would not emit emission lines, the observed double-peaked lines must be formed in regions transparent to the optical continuum. The lines have a symmetric profile because they do not encounter absorbers with a specific distribution of line-of-sight velocities.

## References

1. Y. Tanaka and W.H.G. Lewin in *X-ray Binaries*, eds W.H.G. Lewin, J. van Paradijs and E.P.J. van den Heuvel (Cambridge University Press, Cambridge, 1995), p.126.
2. R. Soria, this volume (2001).
3. R. Soria, K. Wu and R.W. Hunstead, *ApJ*, **539**, 445 (2000).

4. R. Soria, K. Wu and H.M. Johnston, *MNRAS*, **310**, 71 (1999).
5. H.M. Johnston, S.R. Kulkarni and J.B. Oke, *ApJ*, **345**, 492 (1989).
6. J. Smak, *Acta Astron.*, **31**, 395 (1981).
7. R.I. Hynes, et al., *MNRAS*, **300**, 64 (1998).
8. D. Mihalas, *Stellar Atmosphere*, 2nd Edn (Freeman, San Francisco, 1978).
9. W. Tucker, *Radiation Processes in Astrophysics* (MIT Press, Cambridge, 1976).
10. K. Wu, R. Soria, R.W. Hunstead and H.M. Johnston, *MNRAS*, **320**, 177 (2001).
11. E.A. Milne, *MNRAS*, **87**, 43 (1926).
12. G. Dubas, J.-P. Lasota, J.-M. Hameury and P.A. Charles, *MNRAS*, **303**, 139 (1999).
13. J. Smak, *Acta Astron.*, **34**, 161 (1984)
14. D.P. Cox and W.H. Tucker, *ApJ*, **157**, 1157 (1969).
15. D.E. Osterbrock, *Astrophysics of Gaseous Nebulae and Active Galactic Nuclei*. (University Science Books, Mill Valley, 1989).
16. P.J. Callanan, P.A. Charles, W.B. Honey and J.R. Thorstensen, *MNRAS*, **259**, 395 (1992).